THE JOURNAL OF COMPARATIVE NEUROLOGY 429:502–513 (2001)

Projections From the Nucleus of the Basal Optic Root and Nucleus Lentiformis Mesencephali to the Inferior Olive in Pigeons (*Columba livia*)

DOUGLAS R.W. WYLIE*
Department of Psychology, Division of Neuroscience, University of Alberta, Edmonton, Alberta T6G 2E9, Canada

ABSTRACT

The nucleus of the basal optic root (nBOR) of the accessory optic system (AOS) and the pretectal nucleus lentiformis mesencephali (LM) are involved in the analysis of optic flow and the generation of the optokinetic response. Previous studies have shown that the nBOR projects bilaterally to the medial column (mc) of the inferior olive (IO) and the LM projects to the ipsilateral mc. In the present study the retrograde tracer cholera toxin subunit B was injected into either the caudal or rostral mc. From all injections, retrogradely labeled cells were seen in the ipsilateral pretectum along the border of the medial and lateral subnuclei of the LM. Cells were also seen in bilaterally in the nBOR. On the contralateral side, a discrete group of cells was labeled in the rostral margin of the nBOR. These cells were localized in the dorsal portion of the nBOR proper and some were found in the adjacent nBOR dorsalis. On the ipsilateral side, a diffuse group of cells was seen in the caudal nBOR. Most of these cells were in the nBOR dorsalis and outside the nBOR complex in the area ventralis of Tsai and the reticular formation. From the injections into the caudal mc, a greater proportion of labeled cells was found in the LM, whereas a greater proportion of cells was found in the nBOR from the injections into the rostral mc. This differential projection from LM and nBOR to the caudal and rostral mc is consistent with the optic flow preferences of neurons in the mc, and a similar pattern of connectivity has been found in mammalian species. J. Comp. Neurol. 429:502–513, 2001.

Indexing terms: optic flow; optokinetic; vestibulocerebellum; pretectum; accessory optic system; cholera toxin subunit B

Neurons in the nucleus of the basal optic root (nBOR) of the accessory optic system (AOS) and the pretectal nucleus lentiformis mesencephali (LM) are retinal-recipient nuclei (Karten et al., 1977; Reiner et al., 1979; Fite et al., 1981; Gamlin and Cohen, 1988a) and have been implicated in the processing of visual information resulting from self-motion ("optic flow" or "flowfields"; Gibson, 1954). The LM and nuclei in the AOS are principally involved in the generation of visual optomotor responses, including optokinetic nystagmus and the opto-collic reflex, to facilitate retinal image stabilization (birds; Fite et al., 1979; Gioanni et al., 1981,1983a,b; Gioanni, 1988; for reviews, see Simpson, 1984; Simpson et al., 1988a; Grasse and Cynader, 1990). The avian LM is homologous with the mammalian nucleus of the optic tract (NOT), and the nBOR is homologous with the medial and lateral terminal nuclei of the AOS (MTN, LTN) (for reviews, see Simpson, 1984; Fite, 1985; McKenna and Wallman, 1985b; Weber, 1985; Simpson et al., 1988a; Grasse and Cynader, 1990).

Electrophysiological studies have shown that most neurons in the nBOR and LM have large receptive fields in the contralateral eye and exhibit direction selectivity to large-field stimuli rich in visual texture (i.e., random dot patterns or checkerboards). Most neurons in the nBOR prefer large-field stimuli moving either upward, downward, or backward (nasal to temporal; Burns and Wall-

Grant sponsor: Natural Sciences and Engineering Research Council of Canada (NSERC).

*Correspondence to: Douglas R. Wong-Wylie, Ph.D., Department of Psychology, University of Alberta, Edmonton, Alberta T6G 2E9 Canada. E-mail: dwylie@ualberta.ca

Received 14 June 2000; Revised 29 August 2000; Accepted 20 September 2000

man, 1981; Morgan and Frost, 1981; Gioanni et al., 1984; Wylie and Frost, 1990a), whereas most LM neurons prefer forward (temporal to nasal) motion (McKenna and Wallman, 1981, 1985a; Winterson and Brauth, 1985; Wylie and Frost, 1996).

Neuroanatomical studies have shown that the LM projects ipsilaterally, and the nBOR projects bilaterally, to the medial column (mc) of the inferior olive (IO), which in turn projects to the contralateral vestibulocerebellum (VbC) as climbing fibers (CFs) (Arends and Voogd, 1989; Brecha et al., 1980; Gamlin and Cohen, 1988b; Lau et al., 1998; Wylie et al., 1997, 1999b; Crowder et al., 2000). The complex spike activity of Purkinje cells in the VbC, which reflects CF input (Thach, 1967), responds best to particular patterns of optic flow. These neurons have extremely large, virtually panoramic, receptive fields, most of which respond to stimulation of both the ipsilateral and contralateral eyes. In both pigeons and rabbits, it has been shown that cells in the flocculus of the VbC respond best to optic flow resulting from self-rotation about either the vertical axis or an horizontal axis oriented 45° to the midline (Graf et al., 1988; Wylie and Frost, 1993).

These rotational optic flowfields are illustrated in Figure 1A and B. As projected onto a sphere, rotational optic flow consists of laminar motion at the "equator" of the sphere and circular motion at the "pole" (i.e., the axis of rotation). Note that the direction of optic flow is opposite to the direction of rotation. In rabbits, these two cell types are also found in the ventral uvula and nodulus of the VbC (Kano et al., 1990; Wylie et al., 1994, 1995; see also Barmack and Shojaku, 1995). However, in pigeons, cells in this part of the VbC respond best to patterns of optic flow resulting from self-translation along either the vertical axis or a horizontal axis oriented 45° to the midline (Wylie et al., 1993, 1998; Wylie and Frost, 1999a; see Fig. 1, right side). Figure 1C–F shows the optic flowfield resulting from self-translation, which consists of laminar flow along the equator (opposite to the direction of translation) with a "focus of expansion" at one pole (in the direction of translation) and a "focus of contraction" at the opposite pole.

Using retrograde transport from the VbC, it has been shown that the mc has a functional topographical organization (Lau et al., 1998; Wylie et al., 1999; Crowder et al, 2000). This is depicted in Figure 1, which shows a series of coronal sections through the left IO and illustrations of the optic flowfields that maximally excite cells in each region of the mc. Neurons in the medial margin of the mc project as CFs to the Purkinje cells in the flocculus that respond to rotational optic flow, whereas neurons in the lateral margin of the mc provide input to the Purkinje cells in the ventral uvula and nodulus that respond to translational optic flow (Lau et al., 1998). With respect to the rotation cells in the mc, those in the caudal half respond best to rotation about the vertical axis (*rVA* neurons; Fig. 1A) whereas those in the rostral half respond best to rotation about an horizontal axis oriented at 45° ipsilateral (i) azimuth (*r45i* neurons; Fig 1B) (Wylie et al., 1999b). The translation cells are also functionally organized (Crowder et al., 2000). The axis preferences of the translation cells are described with respect to a reference frame where x, y, and z each represent rightward, upward, and forward self-translation, respectively. Cells in the caudal-most margin of the mc respond best to a translational optic flowfield resulting from self-translation along an horizontal axis oriented at 135° contralateral (c) azimuth (*t(x − z)* neurons). This flowfield consists of forward motion in the lateral regions of both visual fields, and a focus of contraction at 45°i azimuth. Moving progressively rostrally in the mc, one encounters *t(+y)*, *t(x + z)*, and *t(−y)* neurons (Fig. 1D–F).

Given this functional arrangement of the mc, one would expect that the caudal and rostral mc would receive differential input from the LM and nBOR. Recall that most LM and nBOR neurons have receptive fields restricted to the contralateral eye, and that most LM neurons prefer forward motion, whereas nBOR neurons prefer either upward, downward, or backward motion (Burns and Wallman, 1981; Morgan and Frost, 1981; McKenna and Wallman, 1981, 1985a; Gioanni et al., 1984; Winterson and Brauth, 1985; Wylie and Frost, 1990a, 1996). From Figure 1 note that, in the caudal mc, the preferred optic flowfield for both *rVA* and *t(x − z)* neurons consists of forward motion in the contralateral hemifield. In contrast, in the rostral mc, the preferred flowfields of *r45i*, *t(−y)*, *t(+y)*. and *t(x + z)* neurons consist of either upward, downward, or backward motion in the contralateral hemifield. Thus, one would expect that the input to the caudal mc would be

Abbreviations

AOS	accessory optic system
AVT	area ventralis of Tsai
CF	climbing fiber
CTB	cholera toxin subunit B
DAB	diaminobenzidine
dc	dorsal cap
dl	dorsal lamella (of the inferior olive)
GLv	nucleus geniculatus lateralis, pars ventralis
GT	tectal gray
IO	inferior olive
LM	nucleus lentiformis mesencephali
LMl	nucleus lentiformis mesencephali, pars lateralis
LMm	nucleus lentiformis mesencephali, pars medialis
LPC	nucleus laminaris precommisuralis
LTN	lateral terminal nucleus
mc	medial column (of the inferior olive)
MLF	medial longitudinal fasiculus
MTN	medial terminal nucleus
nIII	third cranial nerve (oculomotor nerve)
nBOR	nucleus of the basal optic root
nBORd	nucleus of the basal optic root, pars dorsalis
nBORl	nucleus of the basal optic root, pars lateralis
nBORp	nucleus of the basal optic root, proper
NOT	nucleus of the optic tract
PPC	nucleus principalis precommisuralis
R	nucleus raphe
RF	reticular formation
RT	nucleus rotundus
Ru	nucleus ruber
SCI	stratum cellulare internum
SOp	stratum opticum
SP	nucleus subpretectalis
SPL	lateral spiriform nucleus
SPM	medial spiriform nucleus
TeO	optic tectum
VbC	vestibulocerebellum
vl	ventral lamella (of the inferior olive)
vlo	ventrolateral outgrowth
VTRZ	ventral tegmental relay zone

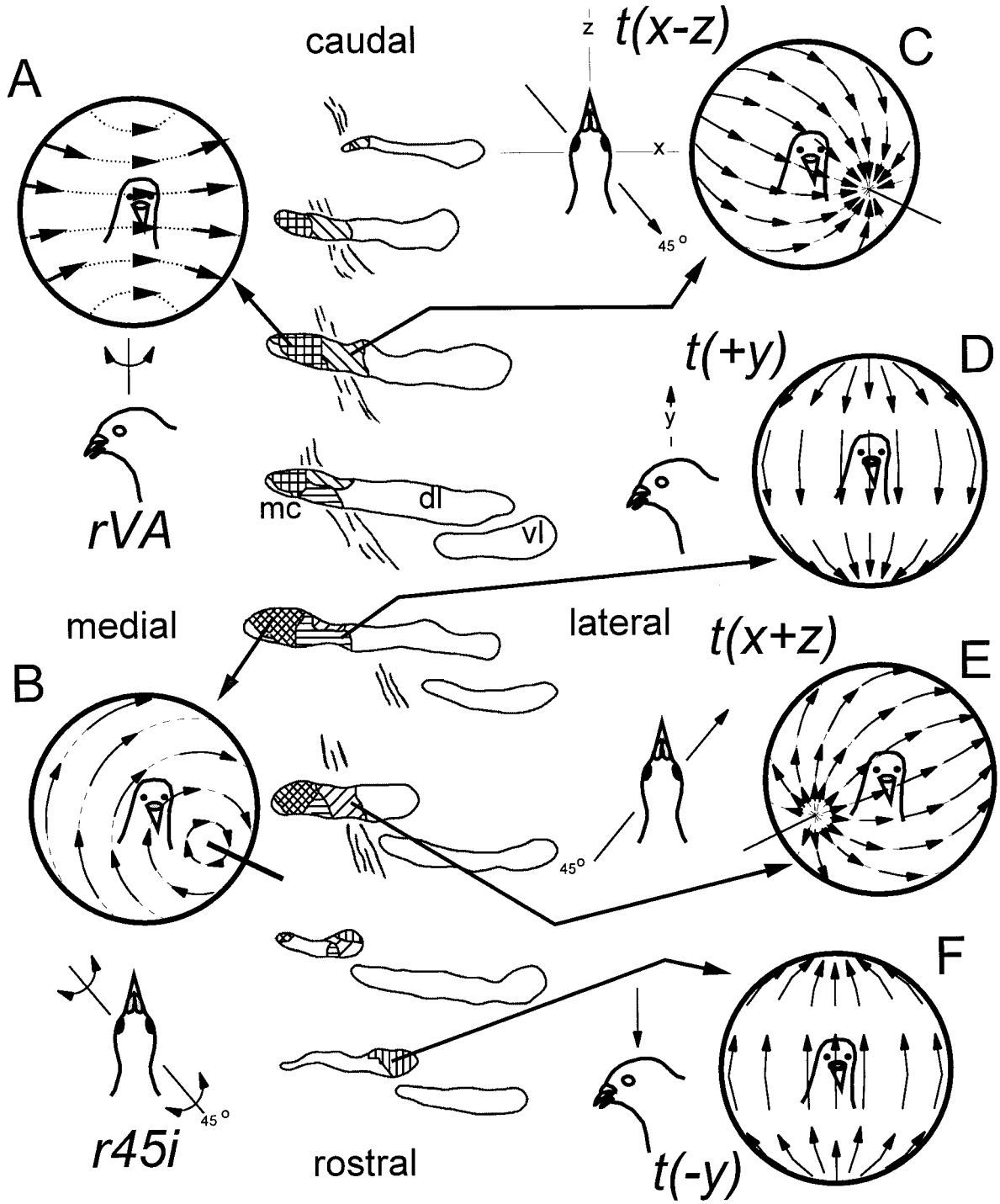

Fig. 1. Topographical organization of the medial column (mc) of the inferior olive (IO) in pigeons. A series of coronal sections through the left IO is shown to indicate the functional topography with respect to the optic flow preferences of neurons (from Crowder et al., 2000). **A–F:** Preferred optic flowfield for each region (i.e., the flowfield that results in maximal excitation for the neurons in each region). Each flowfield is presented as projected onto a sphere surrounding the animal, where the arrows indicate local image motion with the flowfield. The vectors adjacent to each flowfield indicate the direction the animal would translate along (C–F) or rotate about (A,B) to cause the preferred pattern of optic flow. See text for a detailed description.

from the LM primarily, whereas the rostral mc would receive a heavier input from the nBOR.

MATERIALS AND METHODS

Surgery and CTB injection

The methods reported herein conformed to the guidelines established by the Canadian Council on Animal Care and were approved by the Biosciences Animal Care and Policy Committee at the University of Alberta. Silver King and homing pigeons (obtained from a local supplier) were anesthetized with a ketamine (65 mg/kg)/xylazine (8 mg/kg) cocktail (i.m.). Supplemental doses were administered as necessary. The animals were placed in a stereotaxic device with pigeon ear bars and beak adapter so that the orientation of the skull conformed to the atlas of Karten and Hodos (1967). Based on the stereotaxic coordinates of Karten and Hodos (1967), sufficient bone and dura were removed to expose the brain and allow access to the inferior olive with an oblique penetration (10° to the sagittal plane).

Recordings were made with glass micropipettes filled with 2 M NaCl and having tip diameters of 4–5 μm. The extracellular signal was amplified, filtered, and displayed on an oscilloscope. Cells in the IO can be easily identified based on their low firing rate of about 1 spike/sec. After a cell was isolated, the optic flow preference of the neuron was determined by moving a large (90° × 90°) hand-held stimulus in various areas of the visual field and by monitoring responses to translational and rotational flowfield stimuli produced by the planetarium and translator projectors described elsewhere (Wylie et al., 1998; Wylie and Frost, 1993, 1999a,b). After identification of the flowfield preference, the recording electrode was replaced with a micropipette (10–20 μm tip diameter) containing low-salt cholera toxin subunit B (CTB) (1% in 0.1 M phosphate-buffered saline [PBS], pH 7.4); Sigma, St. Louis, MO). The optic flowfield preference was once again determined to confirm the cell type before the solution was iontophoretically injected (+3 μA, 7 seconds on, 7 seconds off) for 3–10 minutes. Following CTB injection, the electrode was left undisturbed for an additional 5 minutes.

Processing for cholera toxin subunit B

After a survival time of 3–5 days, the animals were given an overdose of sodium pentobarbitol (100 mg/kg) and immediately perfused with saline (0.9%) followed by ice-cold paraformaldehyde (4% in 0.1 M phosphate buffer [PB], pH 7.4). The brains were extracted and postfixed for 2–12 hours (4% paraformaldehyde, 20% sucrose in 0.1 M PB) and cryoprotected in sucrose overnight (20% in 0.1 M PB). Frozen sections, 45μm thick, were collected in the coronal plane and then washed in PBS. In some cases, if the perfusion was less than ideal, sections were washed for 30 minutes in a 25% methanol/30% hydrogen peroxide solution to decrease endogenous peroxidase activity.

The CTB protocol used was based on Wild (1993). Tissue was incubated for 30 minutes in 4% rabbit serum (Sigma) with 0.4% Triton X-100 in PBS, followed by goat anti-CHB (1:20,000; List Biological Laboratories, Campbell, CA) for 20–24 hours at 4°C. The sections were then washed with 0.1 M PBS and placed in biotinylated rabbit anti-goat antiserum (1:6,000; Vector, Burlingame, CA) with 0.4% Triton X-100 in PBS for 1 hour. Sections were washed in PBS, then incubated; for 90 minutes in Extravadin peroxidase (1:1,000; Sigma) with 0.4% Triton X-100, and then rinsed again in PBS. The tissue was visualized by using diaminobenzidine (DAB). After a 10-minute incubation in 0.025% DAB and 0.006% $CoCl_2$ in 0.1 M PBS, 0.005% hydrogen peroxide was added, and the tissue was reacted for up to 2 minutes. The tissue was subsequently washed 4–6 times in PBS, mounted on gelatin chrome aluminum-coated slides, lightly counterstained with Neutral Red, and examined by using light microscopy.

Nomenclature

Brecha et al. (1980) divided the nBOR complex into three subgroups based on cell morphology and spatial location (see Figs. 4, 5). The nBOR proper (nBORp) comprises most of the nucleus and consists mainly of large and medium-sized round cells and a smaller number of small spindly cells. The nBOR dorsalis (nBORd) consists of a thin layer of small spindly cells lining the caudal and dorsal margins of the nBORp (Fig. 2B,C). The nBOR lateralis (nBORl) is a small group of cells located dorsal to the stratum opticum (SOp) and lateral to the nBORd/p. McKenna and Wallman (1981, 1985a) have shown that the nBORl is contiguous with and functionally similar to the LM.

In pigeons, the pretectum consists of numerous nuclei, the borders of which are difficult to define. The description by Gamlin and Cohen (1988a,b) has been adopted for the present study. The LM consists of two subnuclei, the LM pars lateralis (LMl) and the LM pars medialis (LMm). Medial to the LMm is a strip of small cells, the nucleus laminaris precommisuralis (LPC), which appears contiguous with the internal lamina of the nucleus geniculatus lateralis, pars ventralis (GLv). Medial to the LPC is the nucleus principalis precommisuralis (PPC), which resides lateral to the nucleus rotundus (RT) (Fig. 2D,E). Ventrally, the LMm, LMl, and LPC course ventral to the nucleus subpretectalis (SP) and posterior to the GLv. The LMm and LMl, although virtually indistinguishable at this point, continue medially as a strip of cells that becomes the nBORl.

RESULTS

CTB was injected in the mc in seven birds. Figure 2A shows a photomicrograph of a typical injection site (from case JB08). From all injections, retrogradely labeled cells were found in the ipsilateral LM and bilaterally in the nBOR complex. Some cells were also found outside the borders of nBOR in the area ventralis of Tsai (AVT) and the reticular formation (RF). The total number of labeled cells in the LM, nBOR, and adjacent AVT/RF varied between 150 and 729 (mean = 402; Table 1). In the contralateral nBOR, a cluster of cells was found rostrally. Most of these cells were found in the dorsal nBORp and some were found in nBORd (Figs. 2B, 4, 5). Fewer cells were found outside the nBOR complex in the adjacent AVT/RF (Table 1, Figs. 4, 5). The labeled cells in the ipsilateral nBOR were found more caudally. They appeared to be smaller than those in the contralateral nBOR, and most were located in the nBORd. Many cells were also found in the adjacent AVT/RF (Table 1, Figs. 2C, 4, 5). Photomicrographs of retrogradely labeled cells in the contra- and ipsilateral nBOR are shown in panels B and C of Figure 2, respectively.

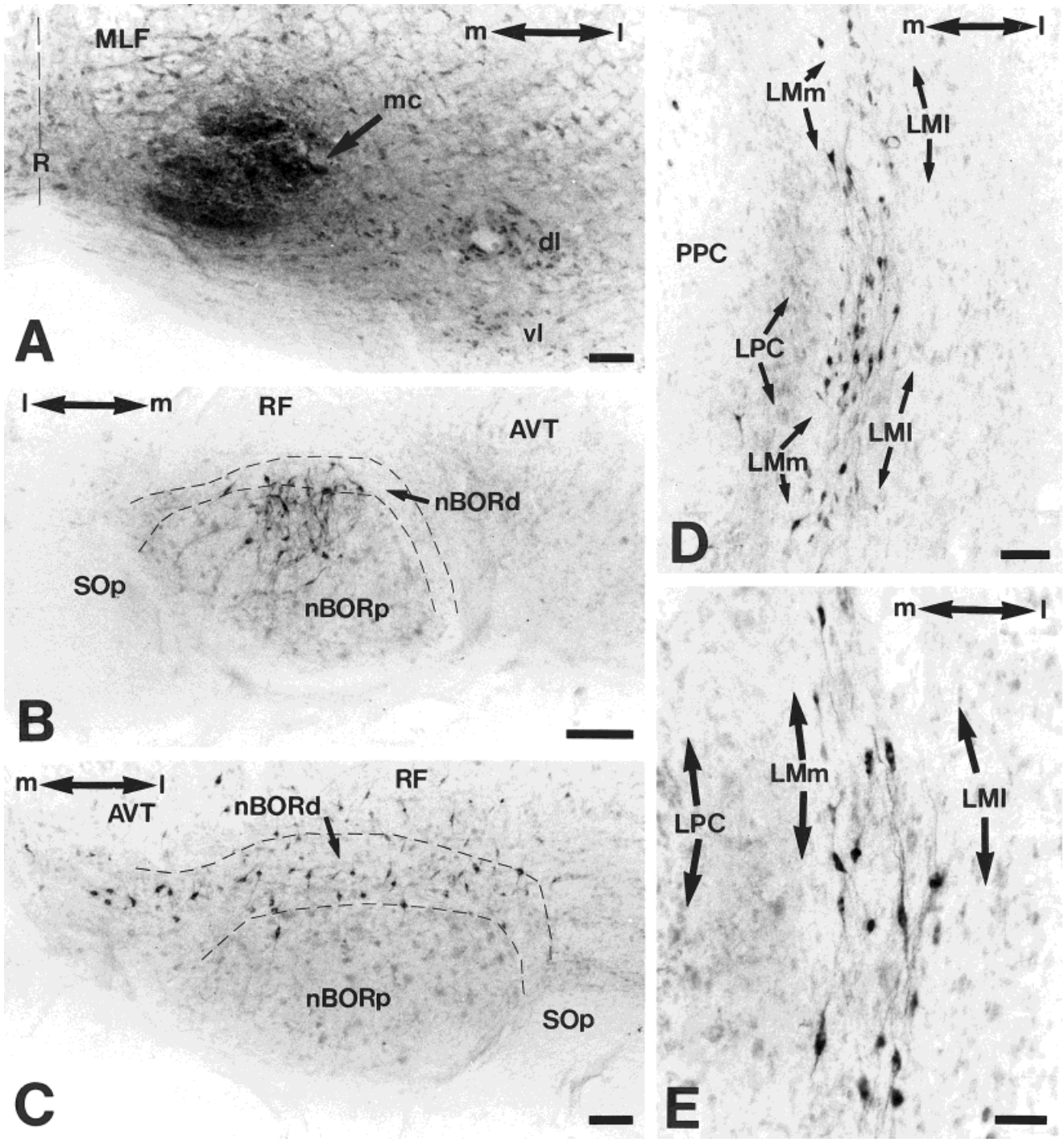

Fig. 2. **A:** Photomicrograph of an injection site in the rostral medial column (mc) of the inferior olive (case JB08). **B–E:** Typical pattern of retrogradely labeled cells in the contralateral nucleus of the basal optic root (nBOR; B), the ipsilateral nBOR (C), and the ipsilateral pretectum (D, E). Note that the bulk of the labeled cells in the pretectum are along the border between the medial and lateral subnuclei of the lentiformis mesencephali (LMm, LMl). See text for additional details. m, medial; l, lateral. Scale bars = 100 μm in A,C,D; 200 μm in B; 50 μm in E.

The labeled cells in the ipsilateral LM appeared as a strip running dorsoventrally through the pretectum. This strip was <150μm in width and was located along the border of LMm and LMl (Figs. 2D,E, 4, 5). At a casual glance, these cells appeared to be located in LMm. However, these cells were large. Both LMl and LMm contain large cells, but the large cells are less common in LMm (Gamlin and Cohen, 1988a,b). Photomicrographs of retro-

TABLE 1. Number and Distribution of Retrogradely Labeled Cells in the Lentiformis Mesencephali (LM), Nucleus of the Basal Optic Root (nBOR), and Area Ventralis of Tsai/Reticular Formation (AVT/RF) from Each of the Seven Cases[1]

Case	NBOR ipsi-	AVT/RF ipsi-	nBOR contra-	AVT/RF contra-	LM ipsi-	Total
JB03 (caudal)	202 (27.7)	82 (11)	201 (27.7)	6 (0.8)	238 (32.6)	729
CtBIO2 (caudal)	198 (27.7)	32 (4.5)	145 (20.3)	3 (0.4)	336 (47)	714
CtBIO18 (caudal)	43 (16.6)	21 (8.1)	49 (18.9)	10 (3.8)	136 (52.5)	259
CtBIO3 (rostral)	55 (36.7)	12 (8)	58 (38.7)	6 (4)	19 (12.6)	150
JB09 (rostral)	59 (22)	24 (8.9)	154 (57.4)	7 (2.6)	24 (8.9)	268
JB07 (rostral)	102 (31.8)	19 (5.9)	139 (43.3)	10 (3.1)	51 (15.9)	321
JB08 (rostral)	114 (30.6)	32 (8.6)	150 (40.3)	7 (1.9)	69 (18.5)	372

[1]Data are numbers, with percents in parentheses.

gradely labeled cells in the LM are shown in panels D and E of Figure 2.

Rostral vs. caudal injections

Three pieces of information were used to determine the location and extent of the injection sites in the IO. First, the optic flow preferences of the neurons at the center of the injection were determined with electrophysiological recordings. Second, the injection sites were examined by using light microscopy, and the extent of the CTB deposits was compared with the known functional topographic organization of the mc from Wylie et al. (1999) and Crowder et al. (2000) (Fig. 3). Figure 3A shows the topographical organization of the mc (from Crowder et al., 2000), and Figure B–H shows reconstructions of the injection sites from each case. The blackened regions indicate heavy CTB deposits, and the gray shaded regions indicate lighter deposits suggestive of spread of the tracer. Comparisons of the reconstructions in B–H with A provide an indication of which areas of the mc were included in the injection site. Finally, the location of anterogradely labeled CFs in the molecular layer of the cerebellar cortex was also considered. If the injection included the *rVA* or *r45i* areas of the mc, anterogradely labeled CFs should be present in the flocculus (Wylie et al., 1993, 1999b; Wylie and Frost, 1993; Lau et al., 1998). If the injection included the translation region, labeled CFs should be present in the ventral uvula and nodulus (Wylie et al., 1993; Lau et al., 1998; Wylie and Frost, 1999a; Crowder et al., 2000).

Previous studies of the ventral uvula and nodulus have shown that the translation neurons are zonally organized (Wylie and Frost, 1999a; Crowder et al., 2000). Considering the complex spike activity of VbC Purkinje cells on the right side of the brain, the zonal organization is as follows: the $t(x - z)$ neurons are found most medially in a zone that abuts on the midline and extends about 0.5 mm laterally; the $t(x + z)$ neurons are found in a zone lateral to this extending from 0.5 to 1 mm lateral to the midline; and the $t(-y)$ and $t(+y)$ neurons are found lateral to these, 1–2 mm lateral to the midline. Although there are no conclusive data in this regard, it has been suggested that the $t(+y)$ neurons are found lateral to the $t(-y)$ neurons (Wylie and Frost, 1999a). In the present study the location of anterogradely labeled CFs in the VbC was measured to provide an indication of the spread of the injection in the mc.

Based on these sources of information, it was concluded that there were three cases in which the injection was in the caudal mc (cases JB03, CtBIO2, and CtBIO18) and four injections in the rostral mc (cases CtBIO3, JB07, JB08, and JB09). The injection sites of the caudal cases are reconstructed in Figure 3B–D. For these three cases, *rVA* neurons were recorded with the injection electrode: the bulk of the injection appeared to be confined to the *rVA* region. For case CtBIO18 (Fig. 3D), anterogradely labeled CFs were found in the flocculus but not the ventral uvula and nodulus, suggesting that the injection was confined to the *rVA* region. For cases JBO3 and CtBIO2 (Fig. 3B,C), in addition to anterogradely labeled CFs in the flocculus, CFs were abundant in the most medial zone of the nodulus (JB03, 0–500 μm; CtBIO2, 150–400 μm from the midline), indicating inclusion of the $t(x - z)$ region of the mc, and some CFs were also seen more laterally in the ventral uvula and nodulus (JB03, 1.0–1.2 mm; CtBIO2, 1.1–1.9 mm from the midline), suggesting encroachment on the $t(+y)$ region of the mc. As the locations of separate *rVA* and *r45i* zones in the pigeon flocculus have yet to be determined, it is possible that all these injection sites encroached on the caudal margin of the *r45i* region of the mc.

The injection sites of the rostral cases are reconstructed in Figure 3E–H. For cases CtBIO3, JB07, and JB08 (Fig. 3E,G,H), *r45i* neurons were recorded at the injection site. Anterogradely labeled CFs were not seen in case CtBIO3. For case JB07, CFs were abundant in the flocculus, but a few were also found laterally in the ventral uvula and nodulus, 1.7–1.9 mm lateral to the midline. This CF labeling probably occurred because the injection included some of the $t(-y)$ and/or $t(+y)$ region of the mc in addition to the *r45i* region. For case JB08, CFs were abundant in the flocculus, and some were also found in the nodulus (1.0–1.7 mm lateral to the midline). Thus, the injection for case JB08 included some of the $t(-y)$ and/or the $t(+y)$ region in addition to the *r45i* region. For case JB09, $t(x + z)$ neurons were recorded at the injection site. A band of CF labeling was found in the ventral uvula and nodulus (1.0–1.4 mm from the midline), and some CF labeling was seen in the flocculus. Thus, in addition to the $t(x + z)$ region, this injection included the *r45i* and perhaps the $t(-y)$ regions of the mc. Again, as the locations of separate *rVA* and *r45i* zones in the pigeon flocculus have yet to be determined, it is possible that all these injection sites encroached on the rostral margin of the *rVA* region of the mc.

Figures 4 and 5 show drawings of series of coronal sections through the nBOR and pretectum from injections into the caudal (case CtBIO2) and rostral (case JB08) mc, respectively. With respect to the distribution of retrogradely labeled cells in the LM and nBOR, there was a clear difference between the rostral and caudal mc injections. This is outlined in Table 1 and illustrated in Figure 6. This figure shows a histogram of the relative number of retrogradely labeled cells found in the ipsilateral LM, contralateral nBOR and adjacent AVT/RF, and ipsilateral nBOR and adjacent AVT/RF, expressed as percentage of the total number of labeled cells for each case. From the injections into the rostral mc, a relatively small number of

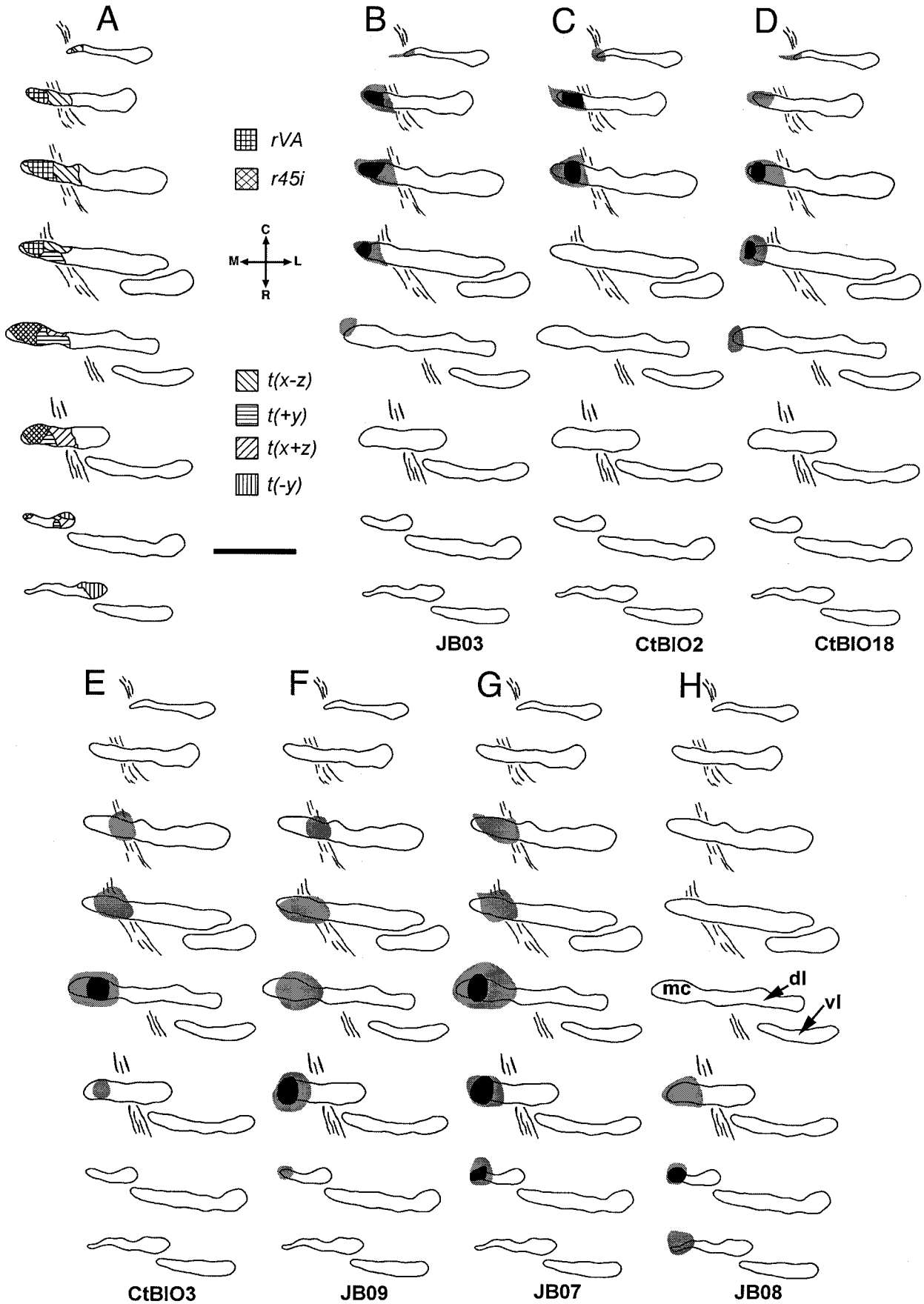

Fig. 3. Injections of cholera toxin subunit B (CTB) in the medial column (mc) of the inferior olive. **A:** A series of coronal sections through the IO illustrating the topographical organization of the mc with respect to the preferred patterns of rotational or translational optic flow (from Crowder et al., 2000; see Fig. 1). **B–H:** Extent of the injection sites from each case. The blackened area indicates the heart of the injection, and the gray area indicates the apparent spread of the tracer. The extent of each injection site can be compared with A to determine which regions of the mc were included in the injection. In B–D the injection was in the caudal mc, whereas in E–H the injection was in the rostral mc. See text for additional details. c, caudal; m, medial; l, lateral; r, rostral. Scale bar = 1 mm.

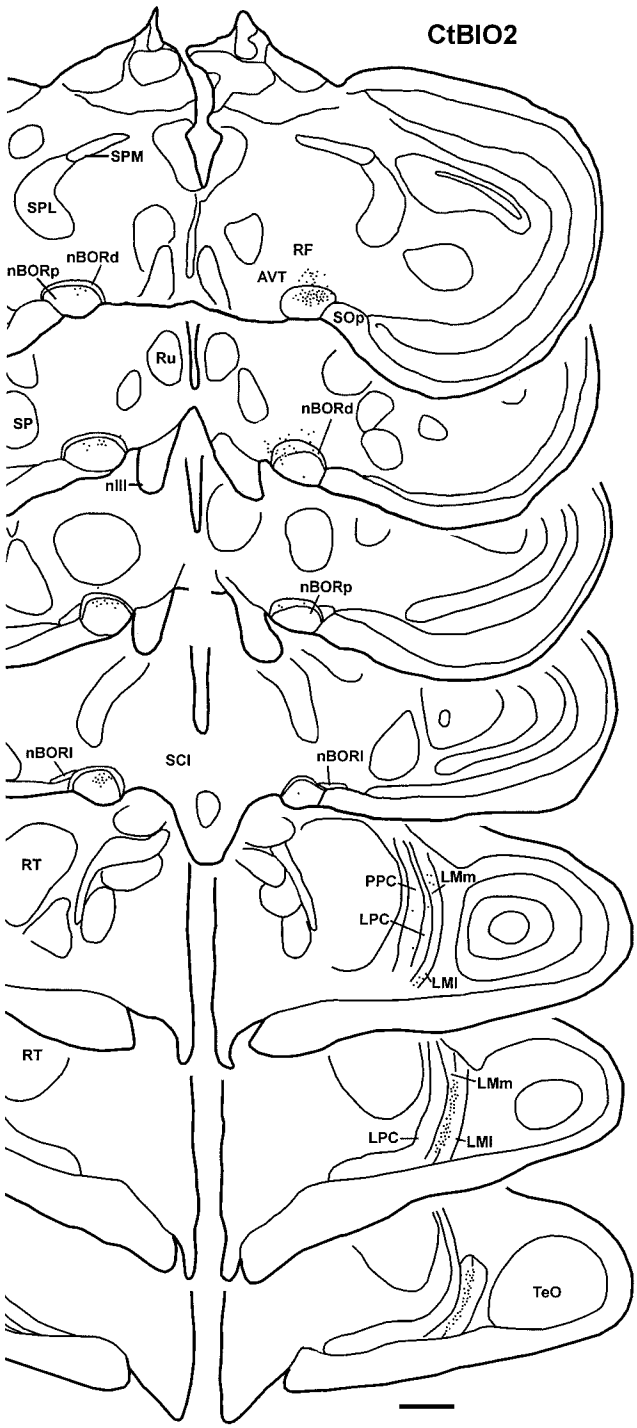

Fig. 4. Projections from the nucleus of the basal optic root (nBOR) and the pretectal nucleus lentiformis mesencephali (LM) to the caudal medial column (mc). Drawings of coronal sections (caudal to rostral) from case CtBIO2 are shown. Each dot represents the location of a retrogradely labeled cell. The injection site is illustrated in Figure 3C. See text for additional details. Scale bar = 1 mm.

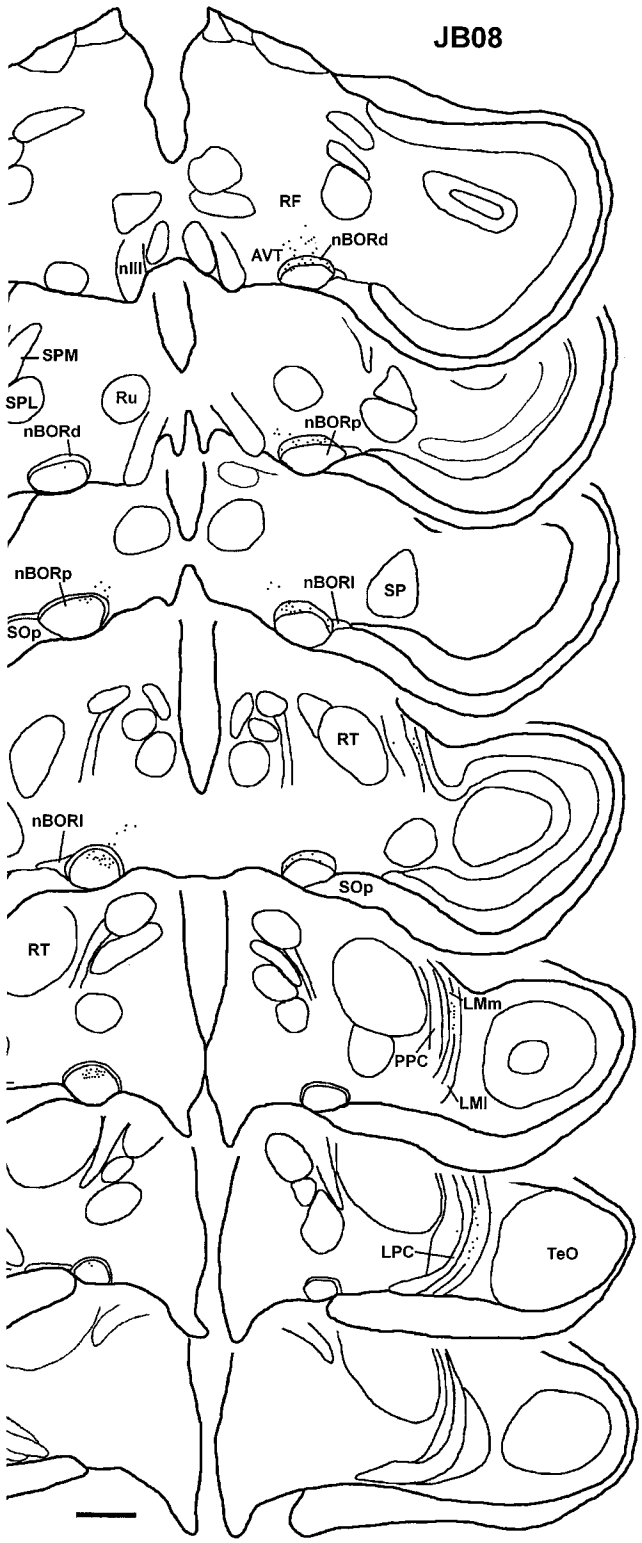

Fig. 5. Projections from the nucleus of the basal optic root (nBOR) and the pretectal nucleus lentiformis mesencephali (LM) to the rostral medial column (mc). Drawings of coronal sections (caudal to rostral) from case JB08 are shown. Each dot represents the location of a retrogradely labeled cell. The injection site is illustrated in Figure 3H. See text for additional details. Scale bar = 1 mm.

labeled cells were found in the LM compared with injections into the caudal mc. The only other apparent difference between the rostral and caudal mc injections was

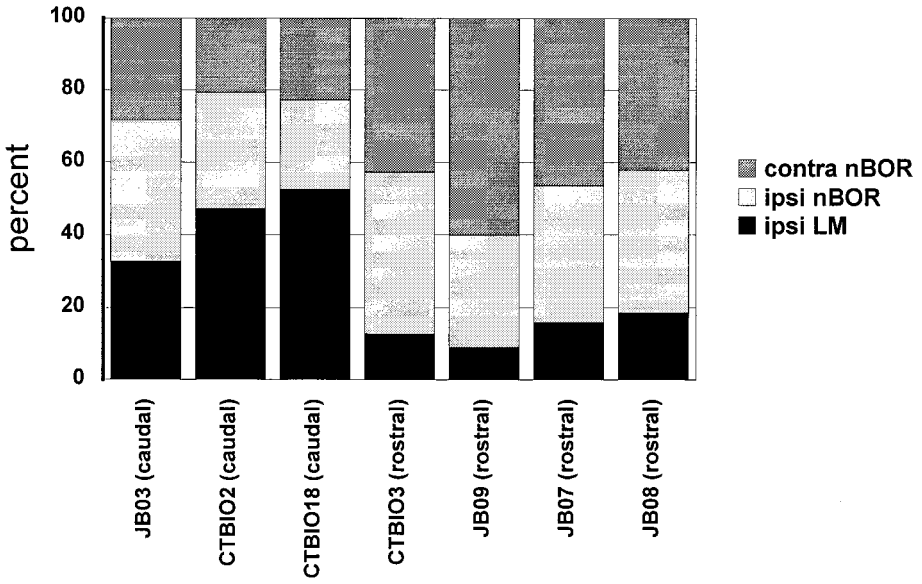

Fig. 6. Percent histogram of the distribution of retrogradely labeled cells from injections into the caudal and rostral medial column (mc). For each case the percentage of cells found in the ipsilateral lentiformis mesencephali (ispi LM; black), the ipsilateral nucleus of the basal optic root (ipsi nBOR; light gray), and the contralateral nBOR (contra nBOR; dark gray) are shown. Cells found in the adjacent area ventralis of Tsai and reticular formation (AVT/RF) are included with those in the nBOR. Note that a smaller percentage of cells were found in the LM after injection in the rostral mc.

with respect to the location of retrogradely labeled cells in the LM. From the rostral mc injections, the labeled cells in the LM were more abundant in the dorsal-caudal regions of LM. The most striking example of this was in case JB08, which is reconstructed in Figure 5. Note the absence of labeling in the LM in the rostralmost section shown. In Figure 4, which shows the retrograde labeling from an injection into the caudal mc (case CtBIO2), there is abundant labeling in the ventral-rostral area of LM.

DISCUSSION

In the present study, after injections of the retrograde tracer CTB into the mc of the IO in pigeons, retrogradely labeled cells were found bilaterally in the nBOR and the adjacent AVT/RF. A bilateral projection from the nBOR to the mc has been noted previously (Brecha et al., 1980; Wylie et al., 1997). In fact, it has been shown that individual nBOR neurons innervate both the ipsi- and contralateral mc (Wylie et al., 1997). From the present study, there are additional details to note. The retrogradely labeled cells in the contralateral nBOR were found further rostral than those in the ipsilateral nBOR. Moreover, the cells in the contralateral nBOR were restricted to a rather tight cluster that included cells in both nBORp and nBORd. The group of labeled cells in the ipsilateral nBOR was more diffuse, and most cells were located in the nBORd. More labeled cells were seen in the AVT/RF adjacent to the nBOR on the ipsilateral side compared with the contralateral side. A group of retrogradely labeled cells was also found in the pretectum, along the border between the LMl and LMm. This was noted previously by Gamlin and Cohen (1988b; see also Clarke, 1977).

It seems that much of the input from the nBOR to the mc arises from nBORd and the adjacent AVT/RF. Previously it has been suggested that the physiological properties of cells in the nBORd and AVT differ from those in nBORp (Wylie and Frost, 1990b, 1999b; Wylie et al., 1999a). Most cells in the nBOR have receptive fields in the contralateral eye, but there are some cells that have receptive fields in both eyes and respond best to particular patterns of optic flow resulting from either self-translation or self-rotation. These binocular units have been found in nBORd (Wylie and Frost, 1990b, 1999b) and the AVT (Wylie et al., 1999a). This is consistent with previous anatomical studies that have shown a projection to the nBORd and AVT from the contralateral nBOR (Brecha et al., 1980; Wylie et al., 1997). Thus, the mc may be receiving input from binocular units in the nBOR complex. However, the binocular nBORd/AVT units show a marked ocular dominance relative to the complex spike activity of neurons in the VbC that receive input from the mc (Wylie and Frost, 1990b, 1999b). Therefore, further binocular integration must take place in the mc. Presumably, for some cell types, the binocular integration would involve inputs from both nBOR and LM. For example, the flowfield that maximally excites the *rVA* neurons in the caudal mc consists of forward motion in the contralateral hemifield and backward motion in the ipsilateral hemifield (Fig. 1A). An mc unit with this flowfield selectivity could be constructed with inputs from the ipsilateral LM (a forward cell) and the contralateral nBOR (a back cell). (However, there are some binocular LM units that respond to rotation about the vertical axis; Wylie, 2000).

The major finding of the present study is with regard to the differences between the distribution of labeled cells in the nBOR and LM from injections into the caudal and rostral mc. A greater number of cells were found in the LM after injections into the caudal mc compared with those injections in the rostral mc. These findings are schemati-

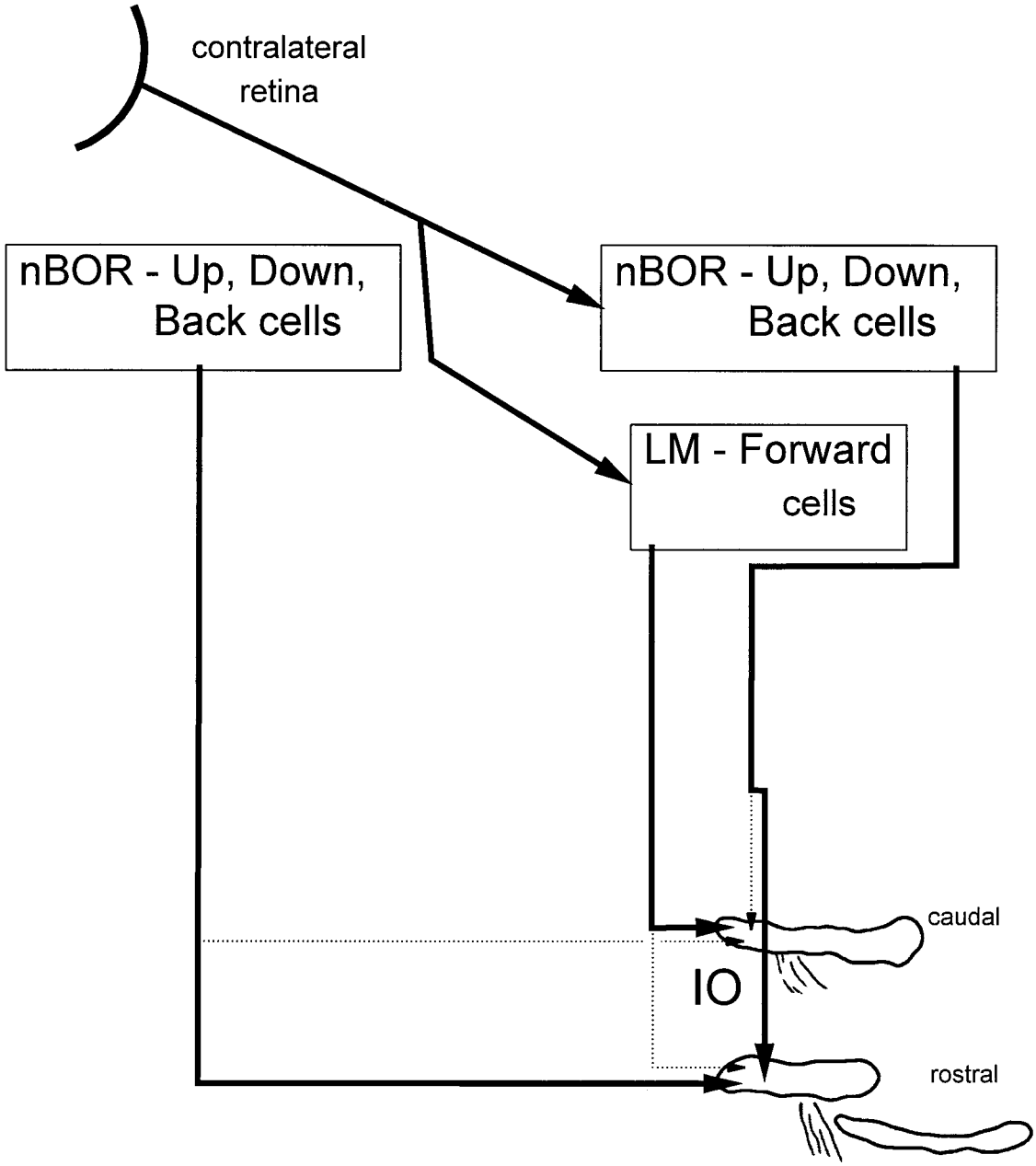

Fig. 7. Schematic illustration of the projection from the nucleus of the basal optic root (nBOR) and the pretectal nucleus lentiformis mesencephali (LM) to the medial column (mc) of the inferior olive (IO). The thicker solid arrows represent heavier projections than the thinner broken arrows. Most cells in the nBOR prefer either upward, downward, or backward motion in the contralateral eye, and most LM cells prefer forward motion in the contralateral eye (Gioanni et al., 1984; Winterson and Brauth, 1985; Wylie and Frost, 1990a, 1996). The nBOR projects bilaterally to the mc, but the projection is heavier to the rostral mc. The LM projects to the ipsilateral mc, but the projection is heavier to the caudal mc.

cally illustrated in Figure 7. The nBOR projects bilaterally to the mc, but the projection is heavier (solid arrows) to the rostral mc and weaker to the caudal mc (dashed arrows). The LM projects to the ipsilateral mc, but the projection is heavier to the caudal mc and weaker to the rostral mc. As outlined in the introduction, this pattern of connectivity is consistent with the direction preferences of neurons in the LM and nBOR and the flowfield preferences of translation and rotation neurons in the rostral and caudal mc. To reiterate, the majority of neurons in the LM and nBOR have monocular receptive fields in the contralateral eye. Most nBOR neurons respond best to either upward, downward, or backward motion (Gioanni et al., 1984; Wylie and Frost, 1990a), whereas most LM neurons prefer forward motion in the contralateral eye (Winterson and Brauth, 1985; Wylie and Frost, 1996). As

shown in Figure 1, in general, the *rVA* and *t(x − z)* neurons in the caudal mc respond best to flowfields that consist of forward motion in the contralateral hemifield, whereas the neurons in the rostral mc respond best to flowfields consisting of upward, downward, and backward motion in the contralateral hemifield.

Comparison with mammalian species

The pattern of connectivity of the pretectal/AOS-olivo-VbC pathway illustrated in Figure 7 seems highly conserved. In the olivo-VbC system in mammalian species, neurons responsive to translational optic flowfields have not been found. However, neurons responsive to the rotational optic flow have been found, and the organization is remarkably similar to that in birds: *rVA* neurons are found in the caudal dorsal cap (dc), and *r45i* neurons are found in the rostral dc and ventrolateral outgrowth (vlo) (Leonard et al., 1988; Ruigrok et al., 1993; Tan et al., 1995). The caudal dc receives input from the NOT (Mizuno et al., 1973; Takeda and Maekawa, 1976; Maekawa and Takeda, 1977; Holstege and Collewijn, 1982), which contains neurons that prefer forward motion (e.g., Collewijn, 1975; Hoffmann and Schoppmann, 1981) and is homologous to the avian LM. Most of the visual input to the rostral dc and vlo arises indirectly from the MTN and LTN via the ventral tegmental relay zone (VTRZ; Maekawa and Takeda, 1979; Simpson, 1984; Giolli et al., 1985; Blanks et al., 1995). The MTN and LTN contain neurons that prefer upward or downward motion (e.g., Grasse and Cynader, 1982, 1984; Soodak and Simpson, 1988) and are considered homologous to the avian nBOR (Simpson, 1984).

The VTRZ could be considered homologous to the avian nBORd/AVT for two reasons. First, Simpson et al. (1988b) showed that neurons in the VTRZ have properties that are similar to those we have described for the pigeon nBORd/AVT. Some VTRZ are binocular and have "bipartite" receptive fields that are maximally responsive to patterns of rotational optic flow. Second, neurons in the nBORd/AVT project to the hippocampal formation as do neurons in the VTRZ (Gasbarri et al., 1994; Wylie et al., 1999a). This AOS-tegmental-hippocampal projection is thought to be important for "path integration" (Wylie et al., 1999a).

Although the pretectal/AOS-IO-VbC pathway seems highly conserved, there is also a direct pathway from the AOS and LM to the VbC in pigeons (Clarke, 1977; Brecha et al., 1980; Wylie et al., 1997). This direct AOS-VbC pathway has been reported in fish (Finger and Karten, 1978) and turtles (Reiner and Karten, 1978) but not frogs (Montgomery et al., 1981). In mammals, this pathway has been reported in the chinchilla (Winfield et al., 1978) but is absent in cats (Kawasaki and Sato, 1980) rats, and rabbits (Giolli et al., 1984).

ACKNOWLEDGMENTS

I thank J. Boman and X. Lu for technical assistance.

LITERATURE CITED

Arends JJA, Voogd J. 1989. Topographic aspects of the olivocerebellar system in the pigeon. Exp Brain Res Suppl 17:52–57.

Barmack NH, Shojaku H. 1995. Vestibular and visual climbing fiber signals evoked in the uvula-nodulus of the rabbit cerebellum by natural stimulation. J Neurophysiol 74:2573–2589.

Blanks RH, Clarke RJ, Lui F, Giolli RA, Van Pham S, Torigoe Y. 1995. Projections of the lateral terminal accessory optic nucleus of the common marmoset (*Callithrix jacchus*). J Comp Neurol 354:511–532.

Brecha N, Karten HJ, Hunt SP. 1980. Projections of the nucleus of basal optic root in the pigeon: an autoradiographic and horseradish peroxidase study. J Comp Neurol 189:615–670.

Burns S, Wallman J. 1981. Relation of single unit properties to the oculomotor function of the nucleus of the basal optic root (AOS) in chickens. Exp Brain Res 42:171–180.

Clarke PGH. 1977. Some visual and other connections to the cerebellum of the pigeon. J Comp Neurol 174:535–552.

Collewijn H. 1975. Direction-selective units in the rabbit's nucleus of the optic tract. Brain Res 100:489–508.

Crowder NA, Winship IR, Wylie DRW. 2000. Topographic organization of inferior olive cells projecting to translational zones in the vestibulocerebellum of pigeons. J Comp Neurol 419:87–95.

Finger TE, Karten HJ. 1978. The accessory optic system in teleosts. Brain Res 153:144–149

Fite KV. 1985. Pretectal and accessory-optic visual nuclei of fish, amphibia and reptiles: theme and variations. Brain Behav Evol 26:192–202.

Fite KV, Reiner T, Hunt S. 1979. Optokinetic nystagmus and the accessory optic system of pigeon and turtle. Brain Behav Evol 16:192–202.

Fite KV, Brecha N, Karten HJ, Hunt SP. 1981. Displaced ganglion cells and the accessory optic system of the pigeon. J Comp Neurol 195:279–288.

Gamlin PDR, Cohen DH. 1988a. The retinal projections to the pretectum in the pigeon (*Columba livia*). J Comp Neurol 269:1–17.

Gamlin PDR, Cohen DH. 1988b. Projections of the retinorecipient pretectal nuclei in the pigeon (*Columba livia*). J Comp Neurol 269:18–46.

Gasbarri A, Verney C, Innocenzi R, Campana E, Pacitti C. 1994. Mesolimbic dopaminergic neurons innervating the hippocampal formation in the rat: a combined retrograde tracing and immunohistochemical study. Brain Res 668:71–79.

Gibson JJ. 1954. The visual perception of objective motion and subjective movement. Psychol Rev 61:304–314.

Gioanni H. 1988. Stabilizing gaze reflexes in the pigeon (*Columba livia*). I. Horizontal and vertical optokinetic eye (OKN) and head (OCR) reflexes. Exp Brain Res 69:567–582.

Gioanni H, Rey J, Villalobos J, Bouyer JJ, Gioanni Y. 1981. Optokinetic nystagmus in the pigeon (*Columba livia*). I. Study in monocular and binocular vision. Exp Brain Res 44:362–370.

Gioanni H, Rey J, Villalobos J, Dalbera A. 1984. Single unit activity in the nucleus of the basal optic root (nBOR) during optokinetic, vestibular and visuo-vestibular stimulations in the alert pigeon (*Columba livia*). Exp Brain Res 57:49–60.

Gioanni H, Rey J, Villalobos J, Richard D, Dalbera A. 1983a. Optokinetic nystagmus in the pigeon (*Columba livia*). II. Role of the pretectal nucleus of the accessory optic system. Exp Brain Res 50:237–247.

Gioanni H, Villalobos J, Rey J, Dalbera A. 1983b. Optokinetic nystagmus in the pigeon (*Columba livia*). III. Role of the nucleus ectomammilaris (nEM): interactions in the accessory optic system. Exp Brain Res 50: 248–258.

Giolli RA, Blanks RH, Torigoe Y. 1984. Pretectal and brain stem projections of the medial terminal nucleus of the accessory optic system of the rabbit and rat as studied by anterograde and retrograde neuronal tracing methods. J Comp Neurol 232:91–116.

Giolli RA, Blanks RHI, Torigoe Y, Williams DD. 1985. Projections of the medial terminal nucleus, ventral tegmental nuclei and substantia nigra of rabbit and rat as studied by retrograde axonal transport of horseradish peroxidase. J Comp Neurol 227:228–251.

Graf W, Simpson JI, Leonard CS. 1988. Spatial organization of visual messages of the rabbit's cerebellar flocculus. II. Complex and simple spike responses of Purkinje cells. J Neurophysiol 60:2091–2121.

Grasse KL, Cynader MS. 1982. Electrophysiology of medial terminal nucleus of the cat accessory optic system. J Neurophysiol 48:490–504.

Grasse KL, Cynader MS. 1984. Electrophysiology of lateral and dorsal terminal nuclei of the cat accessory optic system. J Neurophysiol 51: 276–293.

Grasse KL, Cynader MS. 1990. The accessory optic system in frontal-eyed animals. In: Leventhal A, editor. Vision and visual dysfunction, vol IV. The neuronal basis of visual function. New York: MacMillan. p 111–139.

Hoffmann KP, Schoppmann A. 1981. A quantitative analysis of the

direction-specific response of neurons in the cat's nucleus of the optic tract. Exp Brain Res 42:146–57.

Holstege G, Collewijn H. 1982. The efferent connections of the nucleus of the optic tract and the superior colliculus in rabbit. J Comp Neurol 209:139–175.

Kano M, Kano M-S, Kusonoki M, Maekawa K. 1990. Nature of optokinetic response and zonal organization of climbing fibre afferents in the vestibulocerebellum of the pigmented rabbit. II. The nodulus. Exp Brain Res 80:238–251.

Karten HJ, Hodos W. 1967. A stereotaxic atlas of the brain of the pigeon (*Columba livia*). Baltimore: Johns Hopkins Press.

Karten HJ, Fite KV, Brecha N. 1977. Specific projection of displaced retinal ganglion cells upon the accessory optic system in the pigeon (*Columba livia*). Proc Natl Acad Sci USA 74:1752–1756.

Kawasaki T, Sato Y. 1980. Afferent projection from the dorsal nucleus of the raphe to the flocculus in cats. Brain Res 197:496–502.

Lau KL, Glover RG, Linkenhoker B, Wylie DRW. 1998. Topographical organization of the inferior olive cells projecting to translation and rotation zones in the vestibulocerebellum of pigeons. Neuroscience 85:605–614.

Leonard CS, Simpson JI, Graf W. 1988. Spatial organization of visual messages of the rabbit's cerebellar flocculus. I. Typology of inferior olive neurons of the dorsal cap of Kooy. J Neurophysiol 60:2073–2090.

Maekawa K, Takeda T. 1977. Afferent pathways from the visual system to the cerebellar flocculus of the rabbit. In: Baker R, Berthoz A, editors. Control of gaze by brain stem neurons. Vol 1 in Developments in neuroscience. Amsterdam: Elsevier. p187–195.

Maekawa K, Takeda T. 1979. Origin of descending afferents to the rostral part of the dorsal cap of the inferior olive which transfers contralateral optic activities to the flocculus. A horseradish peroxidase study. Brain Res 172:393–405.

McKenna O, Wallman J. 1981. Identification of avian brain regions responsive to retinal slip using 2-deoxyglucose. Brain Res 210:455–460.

McKenna O, Wallman J. 1985a. Functional postnatal changes in avian brain regions responsive to retinal slip: a 2-deoxy-D-glucose study. J Neurosci 5:330–342.

McKenna O, Wallman J. 1985b. Accessory optic system and pretectum of birds: comparisons with those of other vertebrates. Brain Behav Evol 26:91–116.

Mizuno N, Mochizuki K, Akimoto C, Matsushima R. 1973. Pretectal projections to the inferior olive in the rabbit. Exp Neurol 39:498–506.

Montgomery N, Fite KV, Bengston L. 1981. The accessory optic system of *Rana pipiens*: neuroanatomical connections and intrinsic organization. J Comp Neurol 203:595–612.

Morgan B, Frost BJ. 1981. Visual response properties of neurons in the nucleus of the basal optic root of pigeons. Exp Brain Res 42:184–188.

Reiner A, Karten HJ. 1978. A bisynaptic retinocerebellar pathway in the turtle. Brain Res 150:163–169.

Reiner A, Brecha N, Karten HJ. 1979. A specific projection of retinal displaced ganglion cells to the nucleus of the basal optic root in the chicken. Neuroscience 4:1679–1688.

Ruigrok TJH, Osse RJ, Voogd J. 1992. Organization of inferior olivary projections to the flocculus and ventral paraflocculus of the rat cerebellum. J Comp Neurol 316:129–150.

Simpson JI. 1984. The accessory optic system. Annu Rev Neurosci 7:13–41.

Simpson JI, Giolli RA, Blanks RHI. 1988a. The pretectal nuclear complex and the accessory optic system. In: Buttner-Ennerver JA, editor. Neuroanatomy of the oculomotor system. Amsterdam: Elsevier. p 335–364.

Simpson JI, Leonard CS, Soodak RE. 1988b. The accessory optic system of rabbit. II. Spatial organization of direction selectivity. J Neurophysiol 60:2055–2072.

Soodak RE, Simpson JI. 1988. The accessory optic system of rabbit. I. Basic visual response properties. J Neurophysiol 60:2037–2054.

Takeda T, Maekawa K. 1976. The origin of the pretecto-olivary tract. A study using horseradish peroxidase. Brain Res 117:319–325.

Tan J, Gerrits NM, Nanhoe RS, Simpson JI, Voogd J. 1995. Zonal organization of the climbing fibre projection to the flocculus and nodulus of the rabbit. A combined axonal tracing and acetylcholinesterase histochemical study. J Comp Neurol 356**:**23–50.

Thach WT. 1967. Somatosensory receptive fields of single units in the cat cerebellar cortex. J Neurophysiol 30:675–696.

Weber JT. 1985. Pretectal complex and accessory optic system of primates. Brain Behav Evol 26:117–140.

Wild JM. 1993. Descending projections of the songbird nucleus robustus archistrialis. J Comp Neurol 338:225–241.

Winfield JA, Hendrickson A, Kimm J. 1978. Anatomical evidence that the medial terminal nucleus of the accessory optic tract in mammals provides a visual mossy fiber input to the flocculus. Brain Res 151:175–182.

Winterson BJ, Brauth SE. 1985. Direction-selective single units in the nucleus lentiformis mesencephali of the pigeon (*Columba livia*). Exp Brain Res 60:215–226.

Wylie DRW. 2000. Binocular neurons in the nucleus lentiformis mesencephali in pigeons: responses to translational and rotational optic flowfields. Neurosci Lett 291:9–12.

Wylie DR, Frost BJ. 1990a. Visual response properties of neurons in the nucleus of the basal optic root of the pigeon: a quantitative analysis. Exp Brain Res 82:327–336.

Wylie DR, Frost BJ. 1990b. Binocular neurons in the nucleus of the basal optic root (nBOR) of the pigeon are selective for either translational or rotational visual flow. Vis Neurosci 5:489–495.

Wylie DR, Frost BJ. 1993. Responses of pigeon vestibulocerebellar neurons to optokinetic stimulation: II. The 3-dimensional reference frame of rotation neurons in the flocculus. J Neurophysiol 70:2647–2659.

Wylie DRW, Frost BJ. 1996. The pigeon optokinetic system: visual input in extraocular muscle coordinates. Vis Neurosci 13:945–953.

Wylie DRW, Frost BJ. 1999a. Complex spike activity of Purkinje cells in the ventral uvula and nodulus of pigeons in response to translational optic flowfields. J Neurophysiol 81:256–266.

Wylie DRW, Frost BJ. 1999b. Responses of neurons in the nucleus of the basal optic root to translational and rotational flowfields. J Neurophysiol 81:267–276.

Wylie DR, Kripalani T-K, Frost BJ. 1993. Responses of pigeon vestibulocerebellar neurons to optokinetic stimulation: I. Functional organization of neurons discriminating between translational and rotational visual flow. J Neurophysiol 70:2632–2646.

Wylie DR, De Zeeuw CI, DiGiorgi PL, Simpson JI. 1994. Projections of individual Purkinje cells of physiologically identified zones in the ventral nodulus to the vestibular and cerebellar nuclei in the rabbit. J Comp Neurol 349:448–463.

Wylie DR, De Zeeuw CI, Simpson JI. 1995. Temporal relations of the complex spike activity of Purkinje cell pairs in the vestibulocerebellum of rabbits. J Neurosci 15:2875–2887.

Wylie DRW, Linkenhoker B, Lau KL. 1997. Projections of the nucleus of the basal optic root in pigeons (*Columba livia*) revealed with biotinylated dextran amine. J Comp Neurol 384:517–536.

Wylie DRW, Bischof WF, Frost BJ. 1998. Common reference frame for neural coding of translational and rotational optic flow. Nature 392: 278–282.

Wylie DRW, Glover RG, Aitchison JD. 1999a. Optic flow input to the hippocampal formation from the accessory optic system. J Neurosci 19:5514–5527.

Wylie DRW, Winship IR, Glover RG. 1999b. Projections from the medial column of the inferior olive to different classes of rotation-sensitive Purkinje cells in the flocculus of pigeons. Neurosci Lett 268:97–100.